Vulnerability and Survivability Analysis of Aircraft Fuselage Subjected to Internal Detonations

Young Moon,Geetha Bharatram,Capt. Scott Schimmels,Dr.Vipperla Venkayya

Structures Division, WL/FIBAD
Bldg. 45, Area B
Wright Patterson AFB, Ohio 45433-7542

ABSTRACT

The Air Force, in support of the FAA's (Federal Aviation Administration) Transport Aircraft Survivability Program (TASP), is conducting an extensive test and analysis procedure to determine the vulnerability of commercial airplanes to internal explosions. The program is in response to increasing terrorist activities against civilian targets resulting in loss of life, property damage and general disruptions.

The purpose of this program is to develop survivability strategy to mitigate the effects of internal explosions. Airframe damage is viewed from two aspects, related but requiring different approaches for assessment. The first issue is the damage immediately after explosion and the immediate damage is assessed using simpler local models. The second issue is the safety of post explosion flight which are examined by global models.

Vulnerability maps of the fuselage based on various failure scenarios are being developed for the purpose of examining airframe hardening options.

All analysis results are compared to those obtained from the test program, and the simulations are performed using both MSC/NASTRAN and MSC/DYTRAN.

1. Introduction

The safety of commercial airplanes has become a major concern as a number of airplanes have been brought down by terrorists over the past years. The Federal Aviation Administration (FAA) has been in charge of maintaining the safety of U.S. commercial airplanes against bomb threats from terrorist groups. One approach to make commercial airplanes safer is to develop more advanced bomb-detection apparatus, which necessitates expensive hardware, cost of training personnel, and flight delays. Another drawback with detection devices is that a small explosive may escape the detection device since there is a size limit for detection devices, no matter how sophisticated and sensitive they may be. A bomb, however small, if it is placed at a right place, it can inflict severe damage. Even if the initial bomb damage is small, the subsequent flight may extend the damage and destroy the airplane and passengers.

The idea of hardening airplanes has gained support with the advent of lightweight but high-strength composites. Aircraft hardening needs to start with an understanding of what happens when a bomb detonates in an airplane. An airframe is known to be a very complex structure designed for high efficiency but with low margins of safety and to operate under severe dynamic environments. Thus it is important to know the failure scenario of an in-flight explosion, given the size and location of a bomb under assumed flight conditions. The failure scenario will help determine the safety of airplanes under the assumed flying conditions.

Airframe safety can be viewed from two aspects: One issue is to examine the extent of damage and the aircraft survivability immediately after the explosion. An equally important issue is the aircraft's ability to complete the flight and land safely. It is obvious that the two issues require distinctly different strategies and approaches to address these two situations. Local models and empirical computations are most appropriate to simulate the immediate effects of the explosion on the structure, while global models can be used to predict the behavior of the post explosion flight.

The purpose of this paper is to investigate both issues. Finite element models will be used to simulate and understand the effects of bomb blasts on aircraft structures, using MSC/ NASTRAN for static structural analysis and MSC/DYTRAN for nonlinear transient dynamic analysis. The immediate effects of the explosion on the structure will be evaluated by a local model which represents a portion of the fuselage panel. A global finite element model will be used to study aircraft vulnerability by drawing maps which show the number and locations of elements that fail first in the post explosion flight, and to determine the aircraft survivability.

2. Description of Structures

The fuselage shell of a Boeing 707 is a semi-monocoque type structure composed of skin, longitudinal stringers (longerons), circumferential frames, and bulkheads. The skin is connected to the longerons and frames mostly by rivets. There are 59 longerons at any cross-section of the forward fuselage ranging from 7.22 to 9.60 inches apart circumferentially. Frames are 20 inches apart along the body axis of the airplane. The fuselage structure is strengthened by local frameworks and skin doublers, which reference openings at doors, windows, escape hatches, and other fuselage openings. Figure 1 shows both the plan view and side view of a typical Boeing 707 configuration, giving the production stations in inches. The forward fuselage which extends from Body Station (BS) 360 to BS 600K is used as the global model, and the local panel model covers seven frames from station 540 to station 600F and extends from the passenger floor to the cargo floor. A typical cross-section of a Boeing 707 fuselage is shown in Figure 2 where the locations of longerons and floor stiffeners are presented.

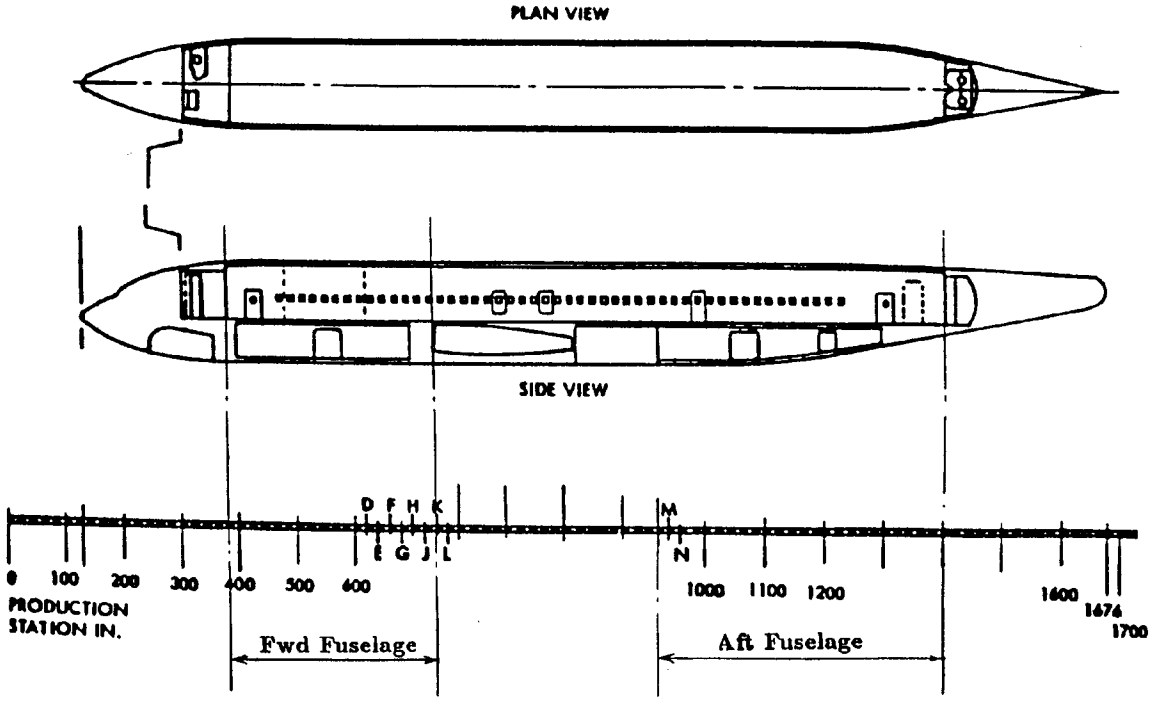

Figure 1. B-707 Aircraft Body Configuration

There are two floors in the fuselage. One is the passenger floor, dividing the fuselage into an upper chamber for passengers, and a lower chamber for cargo. The passenger floor beams support seat tracks upon which passenger seats are mounted. The cargo floor is relatively a rigid member. The cargo bay consists of the passenger floor on the top, a cargo floor at the bottom, right

and left side walls, bulkheads at both ends, and a cargo door at the right.

Aluminium is the material used for the airframe structure. Typical stringers are 7075 rolled hat sections and typical frames are 7075 rolled "Z" sections across the upper crown, with a formed web and angle section on the sides and around the bottom. Figure 3 shows typical stiffener cross-section for frames and stringers. The cross-section shown in Figure 3(a) is for the frames at S-1 through S-14, and from S-15 the height of the stem starts to increase and they are stiffened with one or two angles at the right side of the stem. Typical material for fuselage skins is clad 2024-T3 or T4.

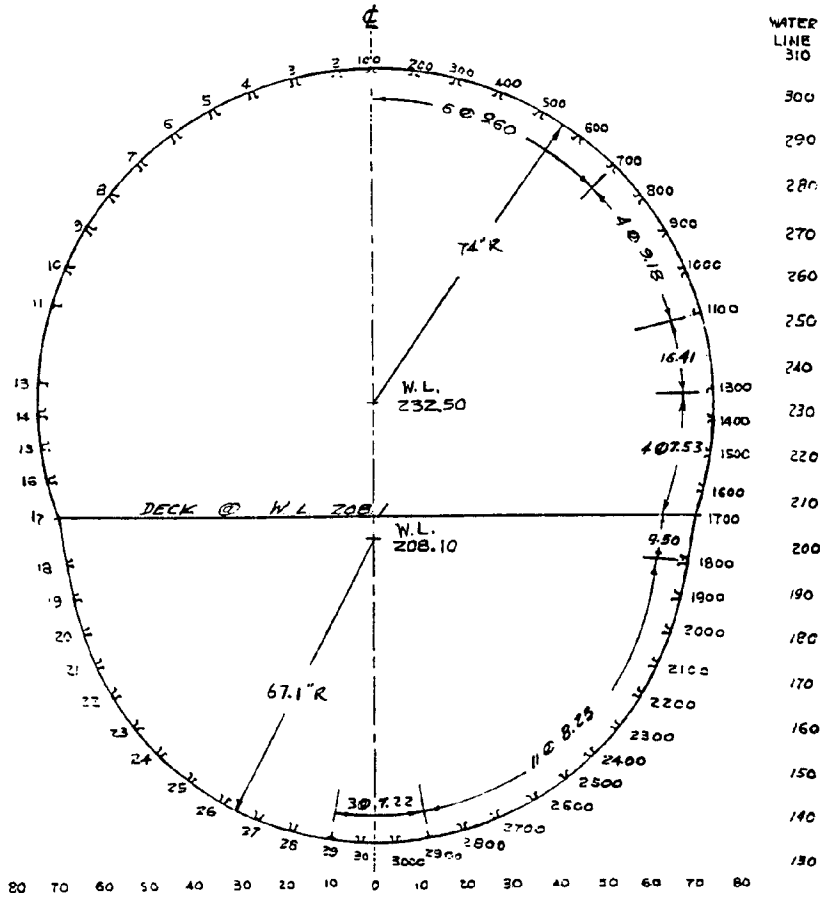

Figure 2. Typical Cross-section with Stiffeners

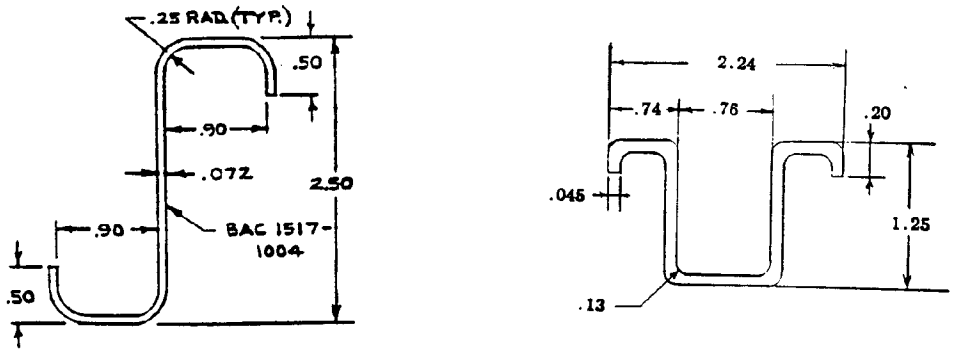

(a) Frame

(b) Longeron

Figure 3. Typical Stiffener Cross-Section (Frame & Longeron)

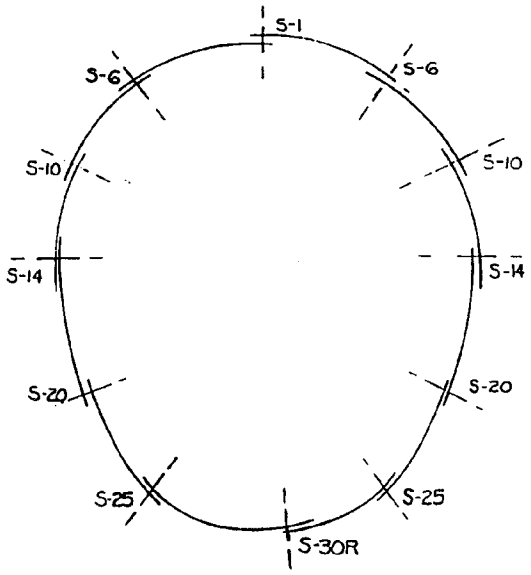

(a) BS 360-600K

Figure 4. Typical Skin Lap Joint Locations

3. Description of Finite Element Models

This section covers the generation of finite element models used for the analysis. The MSC/NASTRAN model of the forward fuselage section is the global model for the construction of the vulnerability map to study the overall behavior of the aircraft after the explosion. The MSC/DYTRAN model is based on the local panel and constitutes the local model for detailed analysis.

3.1 MSC/NASTRAN (Global) Model

The global finite element model employs two types of elements; bar and plate elements. Frames, longerons and all stiffeners are modeled using BAR elements. Their cross-sections are composite areas made of many components which are not uniform and which vary in general from one location to another. BAR elements are also used to model both longitudinal and transverse floor (passenger and cargo) stiffeners, stiffeners at bulkheads, and door (cargo and passenger) frames.

Skins, passenger and cargo floors, and bulkheads are modeled with isoparametric membrane-bending plate elements (CQUAD4 and CTRIA3).

The source of information for the generation of the MSC/NASTRAN finite element model is the four-volume stress report in Reference 1 which contains coordinates of points where frames meet longerons for outer geometry of the aircraft, and some details of frame and longeron properties. A very useful source of information comes from an actual forward fuselage section brought into Area B, WPAFB, Ohio. Many detailed section properties and dimensions not found in Reference 1 were identified and measured from this actual airplane structure.

The finite element model shown in Figure 5 is the basis for the analysis and consists of 4,508 GRIDs, 5,044 CBARs and 4,880 plate elements. The model is assumed as cantilevered at BS 600K for boundary conditions. Therefore, all the grid points at the bulkhead (BS 600K) are constrained in all directions, since it is known that the airplane in flight deflects with respect to the roots of the wing because of the heavy structure in the body around the wing roots. The effect of the cockpit on the model is accounted for by taking the total mass (COMN2) of the cockpit at the CG of the cockpit and connecting the mass to the grids at BS 360 by rigid bars (RBE3).

The loading conditions applied for analysis are internal pressure of 8.6 psi, gravity loading, drag, and various combinations of these three loads.

The concept of vulnerability map is based on the premise that the vulnerability of the fuselage varies both longitudinally and transversely. Associated with each point in the fuselage, a charge size that triggers failure when exploded is the basis for the vulnerability map. This model is intended for analyzing global effects on the aircraft such as overall stress/strain distribution, deformation pattern and generating a vulnerability map. The overall behavior of the aircraft for post explosion flight can be well simulated using the global model.

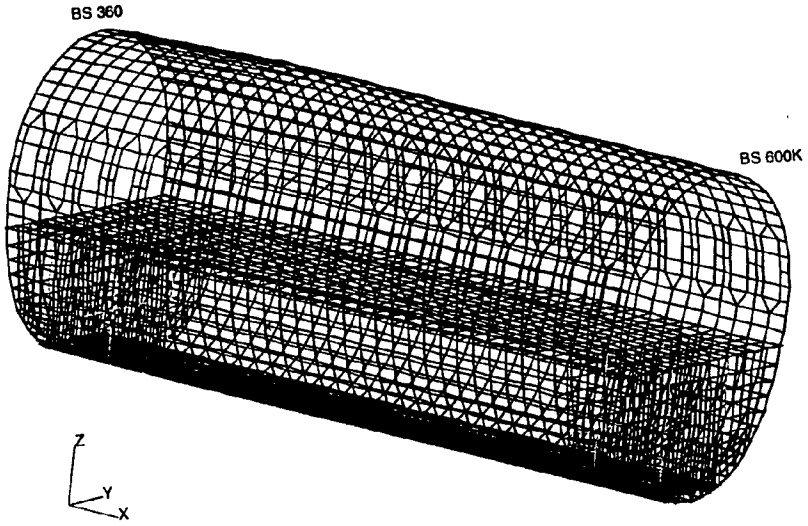

Figure 5. Finite Element Model of Forward Fuselage

3.2 MSC/DYTRAN (Local) Model

Since the beams in the global finite element model are modeled as 1-D elements, failure of the beams such as buckling and crippling of the frames can not be visualized or simulated. Also, a permanent joint exists between the skin and the frame as they share the same grid point. This makes it impossible to simulate the separation of the skin from the frame. For a detailed analysis such as buckling of frames, joint failure analysis, etc., local models are more suitable. Such a model can simulate the sequence of failure in the structural components during a blast explosion and identify the failure modes of the fuselage during the event. The basic DYTRAN model consists of fluid inside the fuselage and structural model surrounding it. The fluid is represented by Eulerian model and the structure by Lagrangian model.

3.2.1 Lagrange Model

The transient dynamic response analysis is performed on the B-707 panel model using the hydrocode, MSC/DYTRAN [2]. In the simulations performed, the code is operated in the Arbitrary Lagrange Euler (ALE) mode. That is, as the Lagrangian structure deforms, the Eulerian grid is displaced to match the Lagrangian grid at the points along the interface between the two.

The analytical Lagrange model of the panel consists of shell (CQUAD4) elements for the skin as well as the frames and longerons as shown in Figure 6. Every rivet position is modeled with a grid point. The Lagrange model spans seven frames from frame station 540 to frame

station 600F and extends from the passenger floor to the cargo floor. Stringers 17 through 27 are modeled in the panel. The transverse frame height varies from 7" (at stringer 17) to 3" (at stringer 27). Lap joints are present at stringer S-20 and S-25. Simply supported boundary conditions are applied at the top (S-17) and bottom (S-27) of the panel. Springs (CELAS) are defined at frame station 540 and frame station 600F in all three coordinate direction. The passenger and cargo floor are relatively rigid members, therefore simply supported boundary conditions at the top and bottom of the panel are adequate.

The panel model consists of three parts: the skin model, the frame model, and the longeron model. The three models are combined together, but the nodes are not equivalenced. Therefore at locations where a rivet position exists a pair of grid points exist with the same coordinates but different node numbering. These nodes are then defined as a breakable joint with the BJOIN card.

There are a large number of various joint types used in the fuselage: (1) Butt Joints which run along the circumference of the fuselage to connect sections of the fuselage at the manufacturing breaks, (2) Lap Joints to connect stiffened panels, (3) Skin to Frame Joints, (4) Skin to Longeron Joints, and (5) Frame to Longeron Joints.

The joints described above are primarily permanent fasteners such as rivets. The main disadvantage of these joints is that the tensile and fatigue strengths of rivets are lower than bolts and screws. Therefore high tensile loads may pull out the clinch, or severe vibrations may loosen the fastening. When a blast pressure is applied on the walls of the fuselage, essentially a large tensile force is applied to the rivets, possibly causing the rivets to fail in succession (unzipping effect). To simulate and understand this kind of local failure mechanism, MSC/DYTRAN was used to show the unzipping of the frames and longerons from the skin, along with their buckling, when subjected to a blast loading.

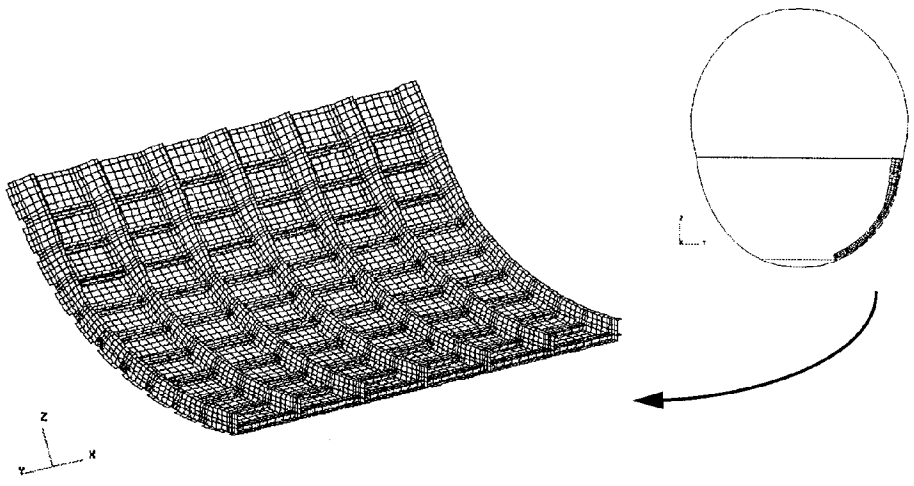

Figure 6. B-707 Panel Model

The rivets used for the construction of the panel are a standard 0.187" diameter fastener made of Al 2017 material. The rivet material has a yield strength of $\sigma_y = 40ksi$ and an ultimate strength of $\sigma_u = 55ksi$. 7Figure 8 shows the dimensions of a standard rivet in the B-707 construction. As shown in the figure, the rivets are flush mounted.

Standard methods of stress analyses for riveted joints considers two primary types of failure, namely the shear of the shank of the rivet and the bearing or compressive failure of the metal at the point where the rivet bears against the connecting sheet or plate. However, rivets in aircraft are generally designed for small tension loads, for example, the skin on the upper surface of the wing, due to the upward suction air forces, places the rivets that hold the skin to the stringers and ribs in tension. During a blast loading, the primary loading on the joints is tensile, and, therefore it is important to calculate the rivet strength in tension for the panel.

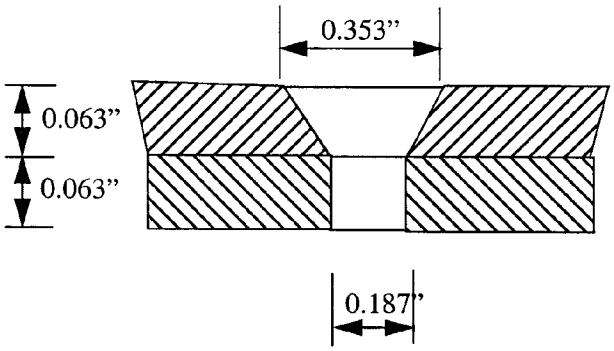

Figure 7. Rivet Dimension

The force that the rivet can withstand is computed by a program developed by Venkayya, V.B, et. al. [3]. The force on the rivet is computed to be 2,950 *lbs*. This computed force is used as the failure criterion to be satisfied for the numerical joint analysis performed on the panel. This is a preliminary estimation of the rivet strength.

3.2.2 Euler Model

An Eulerian mesh was generated extending from the outer skin structure to the center of the fuselage as shown in Figure 8. The Euler mesh was generated from the MSC/PATRAN phase 1 model of the Lagrange structure. The outer surface of the Euler mesh matches the Lagrange mesh at all grid points, and consists of CHEXA elements. An ALE coupling surface was established between the Euler mesh and the Lagrangian structure. The ALE surface was defined using CQUAD4 elements. This surface acts as the fluid structure interaction boundary. The blast wave travelling through the Euler medium transmits impulse to the ALE surface, which in turn loads the Lagrange structure.

In the Euler model, the passenger and cargo floor were considered as rigid boundaries,

therefore in the Euler mesh they were represented as fully reflective surfaces using the WALLET card in MSC/DYTRAN. The sides of the model at frame station 540 and frame station 600F were defined as flow boundaries using the FLOWDEF card. This allows for free flow out of the Euler mesh at these locations.

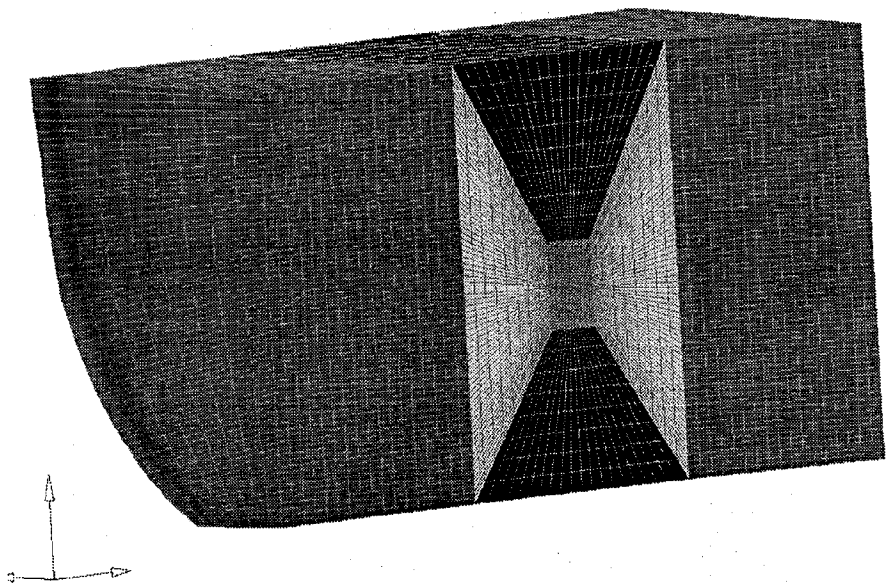

Figure 8. Euler Model for the Panel

4. Global Model Analysis Results

4.1 Finite Element Model Validation

The only test data available are those from blast tests that were conducted using a series of charges placed at different locations. Therefore, the validation of the MSC/NASTRAN finite element model was performed, first of all, by generating an MSC/DYTRAN model of the cargo bay which uses the MSC/NASTRAN model as a Lagrange model. The Euler model was generated based on the Lagrange structure. Analysis results obtained from this MSC/DYTRAN model were compared to test data. Figure 9 shows locations of two gages: gage A for accelerometer and gage P for pressure measurement. The impulse of structure was obtained by computing the area under the pressure-time history curve and shown in Figure 10(A). Figure 10(B) compares absolute displacements at the location of accelerometer A. Comparisons of both impulse and displacement between tests and analysis predictions prove the model satisfactory.

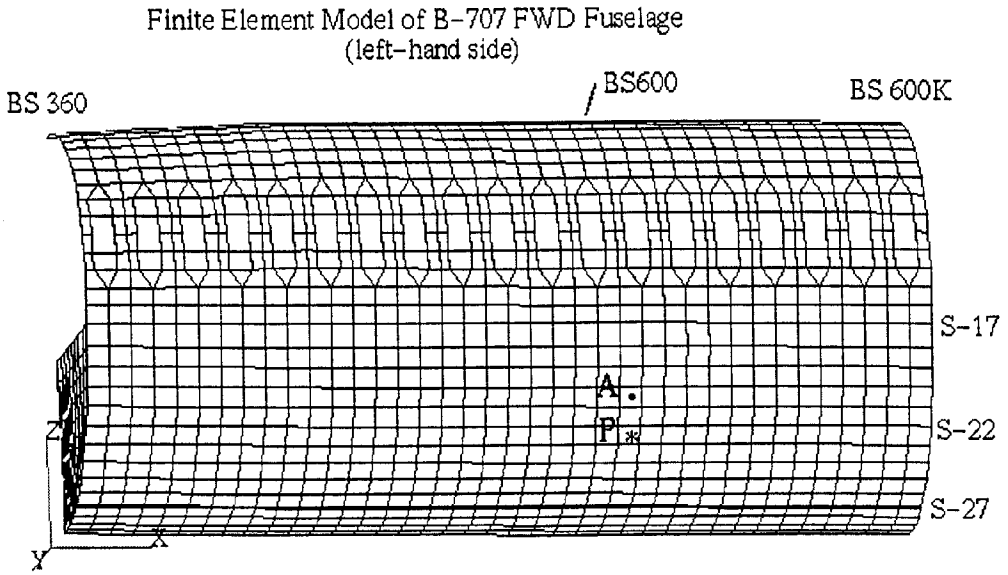

Figure 9. Location of gages

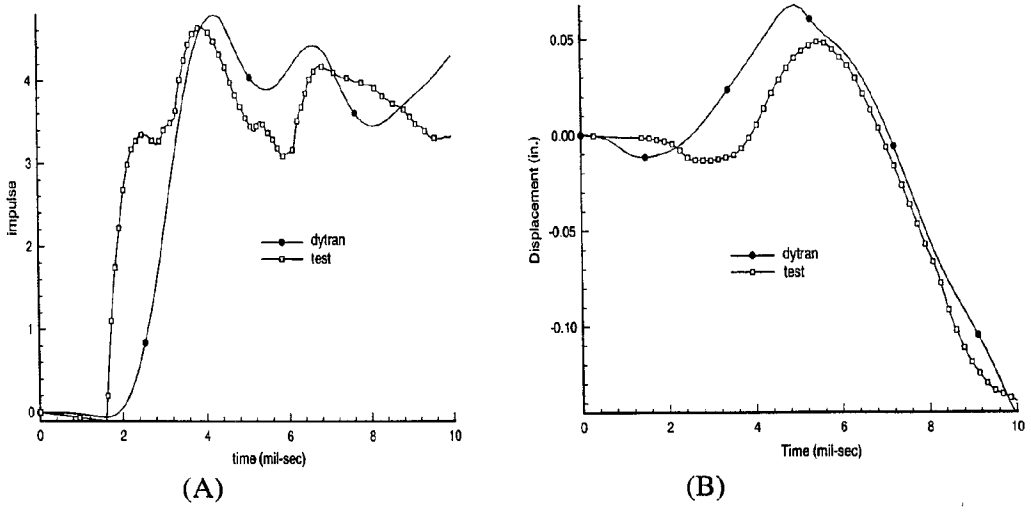

Figure 10. Comparison of Analysis to Test

4.2 Vulnerability Analysis Results

Since the vulnerability of an aircraft to bomb explosions inside the cargo depends on the bomb size and location, and also on the time of explosion and the flight condition, it is impossible to predict the failure scenario of an in-flight explosion. However, under assumed damaged conditions which include types and locations of elements failed, it is possible to write the failure scenario of an in-flight explosion. The failure scenario can be used to determine the effect of failed elements to the other parts of the aircraft (vulnerability), and to see if the aircraft can make it to the nearest airport (survivability). As this scenario deals with an airplane in the post-explosive environment, the analysis is limited to a series of static analysis.

The procedure to investigate the vulnerability of an aircraft when an explosive is detonated in the cargo bay of an airplane follows a parametric study. This parametric study was performed first with one section of frame between passenger and cargo floor at BS 600 failed. The finite element model was run to obtain element stresses of the model under the four loading conditions: (1) 8.6 psi internal pressure, (2) gravity, (3) 8.6 psi and 1 g load, and (4) 8.6 psi and 2.5 g load. For each loading, elements were checked to assure that any element stress should not exceed the element maximum stress allowable. Any element showing higher stress than the maximum allowable value was eliminated from the model, and the model was resubmitted. The procedure was continued until none of the existing elements yielded. And the same procedure is applied to other types of elements and finally to the combination of different elements. An aircraft is not survivable when elements keep failing and unzipping of elements occurs.

The following four cases are presented here to illustrate the procedure. In all cases the yield stress of the material was chosen as the maximum allowable stress; 70 ksi for frames and stringers, and 47.5 ksi for plate elements. Element stresses were evaluated under the internal pressure of 8.6 psi and 1 g load only. The other load cases can be studied in a similar method. Case 1 in Figure 11 starts with one frame (shown in dark line) failed. The analysis shows two stringers (shown with "X") have yielded. When the analysis was continued with the two stringers out, the maximum tensile stress of bar elements was found to be 56.9 ksi and the maximum von Mises stress of plate elements was 25.5 ksi, under the combined 8.6 psi and 1 g load. Since all element stresses are under the yield stress of the material, analysis was stopped. In a similar way, Case 2 was run with three frames (shown in dark lines) failed. The first analysis run indicated that four stringers (shown with "X") failed, and the second analysis run, where the four stringers failed in the first run were taken out from the model, presented two additional stringers (shown with "Y") failed. After this, the third analysis indicates that the maximum bar stress was 57.3 ksi and the maximum von Mises stress was 34.4 ksi.

Cases 3 and 4 in Figure 12 were studied for comparison with Cases 1 and 2. The only difference is that Cases 3 and 4 have twenty more stringers (shown in dark horizontal lines) failed. The failure patterns in Cases 3 and 4 are same as those in cases 1 and 2, respectively. This was expected because the internal pressure is supported mainly by circumferential frames and longerons support gravity. And the maximum element stresses in Cases 3 and 4 are a little lower than those in Cases 1 and 2.

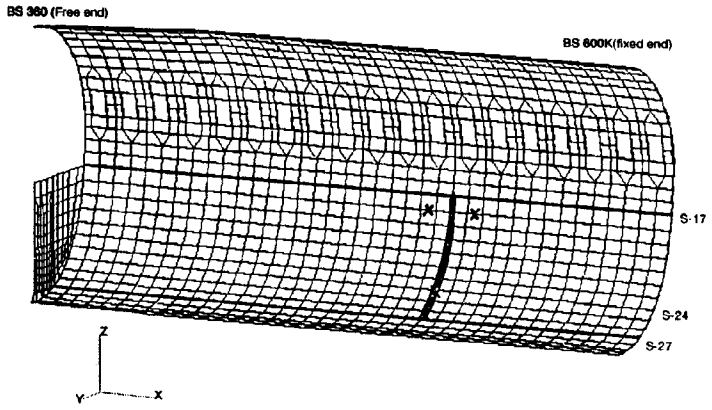

Case 1

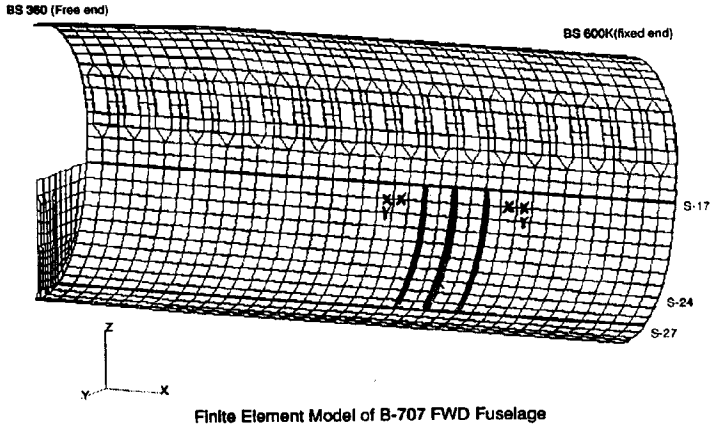

Case 2

Figure 11. Vulnerability Map: Case 1 & Case 2

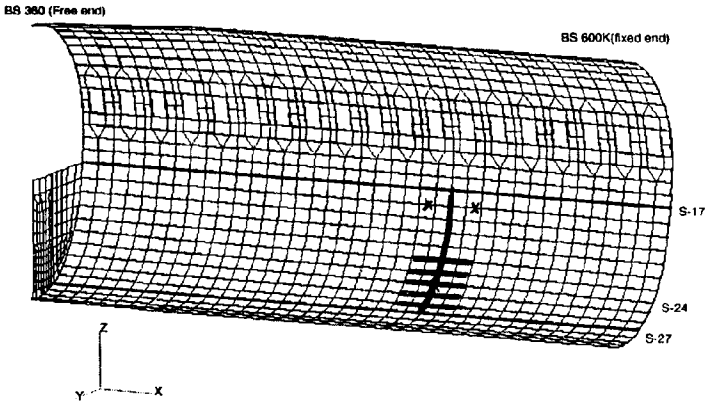

Finite Element Model of B-707 FWD Fuselage
(left-hand side)

X: at BS600 and S-24

Case 3

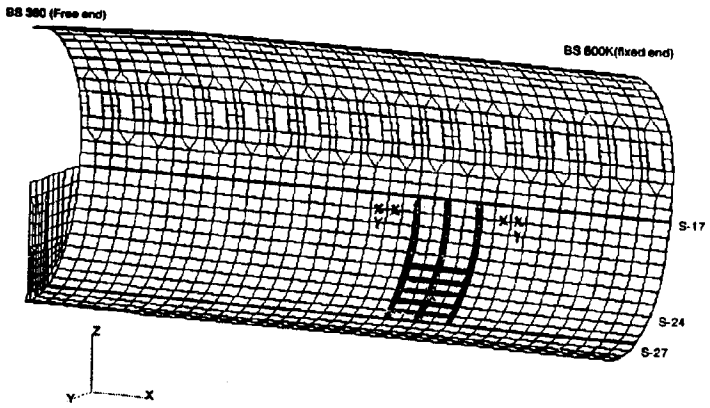

Finite Element Model of B-707 FWD Fuselage
(left-hand side)

X: at BS600 and S-24

Case 4

Figure 12. Vulnerability Map: Case 3 & Case 4

5. Local Model Analysis Results

Analysis of the B-707 panel model has not been completed. The fluid/structure interaction between the panel and the Euler is not working properly. The Euler model (air) runs fine, but when combined with the ALE surface to the Lagrange panel, gives rise to very high energy at the BJOIN elements, causing the immediate failure of the joints. The problem is being addressed. Results from the simulation performed on the Euler model alone are presented in this paper.

Some of the problems experienced while modeling the panel are discussed below. One of the problems may be in the overlapping Quads, i.e. the elements joined by the BJOIN. Since all of the Lagrange model is defined as ALE surface, also all overlapping Quads (having initially identical geometric positions albeit defined on different GRID numbers) will be part of the ALE. This causes a problem because ALE does the following:

For each node of an Euler ALE surface element, Euler looks for a corresponding node in the Lagrange part. Once it finds such a node, it continues on, and Euler looks for a next Lagrange node coinciding with the next node on the Euler surface. Once it has found one corresponding Lagrange node for each of the Euler nodes, it starts to compute Euler pressure forces, and attributes them to the Lagrange nodes just found. Euler does not check whether the nodes found belong to the same or different Lagrange element.

Depending upon internal sequences for storage and loop counts, the ALE Euler may attribute forces partly to one and partly to the other quad element. It does not by definition load them on either one or the other of the overlapping quads, because Euler would not know the difference. In fact, having initially the same coordinates, it is not even possible to tell which one of the overlapping quads is nearest to the "inside" of Euler. Because of this, Euler forces attributed, for all practical purposes are "arbitrary" in each one of the quads. Thus there will be non-equilibrium forces acting both on the overlapping quads and on the nodes of each one of the quads because of the uncertain way in which Euler may attribute the nodal forces.

A secondary problem is more fundamental in the modeling. Assuming that the above problem would not exist, then all would go well until a BJOIN fails. But, then there are two separate nodes where before they were separate but coinciding. From then on, Euler would not know which one of those nodes to follow, since both were defined to control the ALE, and after break-up they will go off in different directions.

This problem has been addressed and different property ids have been defined for the quads that have the same location but different grid ids. Only one of the duplicate quads has been included in the ALE surface definition. This modification has not completely resolved the energy rise in the Lagrange model.

The Euler model alone was run. Blast wave progression are plotted in Figure 13. Figure 13 plots the wave propagation at timesteps 2.0, 7.0 and 10.0 milliseconds. The blast wave reaches the cargo and passenger floor at time 2.0 milliseconds. These are the points closest to the charge. Reflections of the passenger and cargo floor are shown at time 7.5 milliseconds.

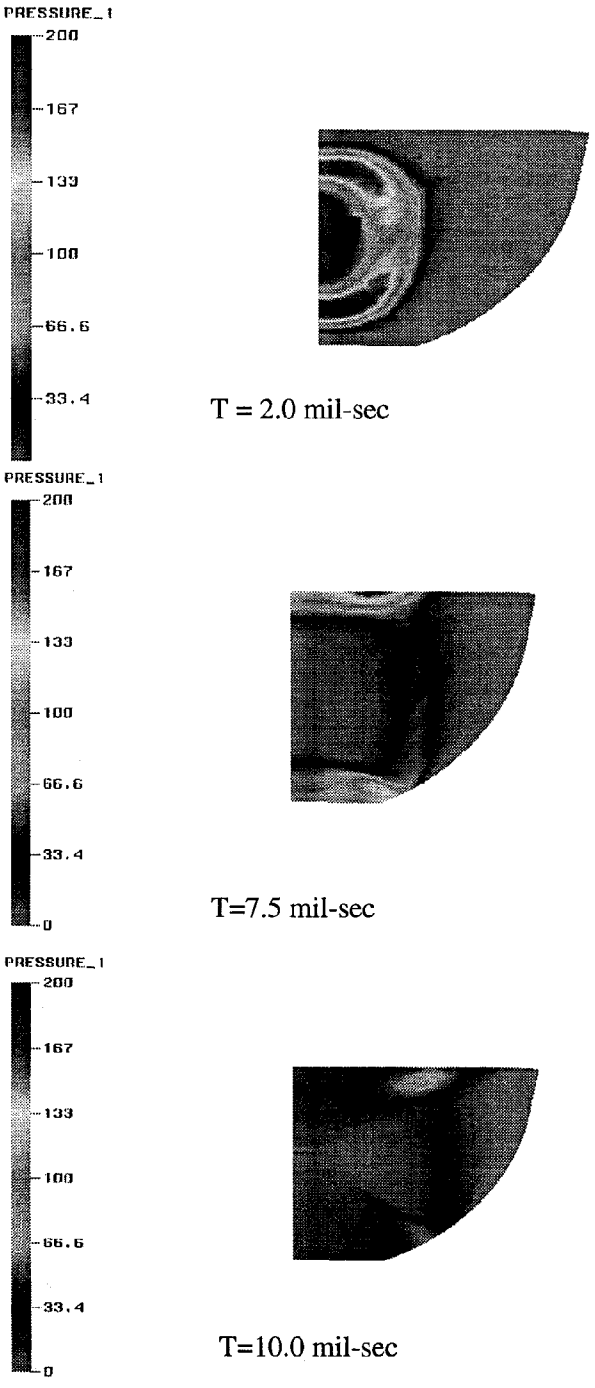

Figure 13. Blast Wave Progression in The Euler Model

6. Summary and Conclusions

The Air Force has participated in the FAA's Transport Aircraft Survivability Program and conducted an extensive test program and collected a large amount of test data on the structural response to the internal explosions. The test data available have been used to modify finite element models. The purpose of the present study is to investigate the extent of the immediate damage due to bomb blasts inside the cargo bay, and to predict the behavior of the post explosion flight.

For assessment of immediate damage, MSC/DTTRAN models of a panel and the entire forward fuselage are examined for comparison with test data. The forward fuselage data are in reasonable agreement with the test data. The data from the local panel model needs further assessment because of the current deficiencies of MSC/NASTRAN in modeling joint failure.

References

1. "Fuselage Stress Analysis for 700-300 and -400 SEries Airplane," Vol. I, II, III, and IV, 1958, Boeing Airplane Co., Seattle, Wash.

2. MSC/DYTRAN - A 3D Code for Explicit Transient Dynamics. The MacNeal-Schwendler Corporation, Los Angeles, CA.

3. Venkayya, V.B, Eimermacher, J.P., and Kinzing, W., "Recessed head fastener strength evaluation program", Technical Memorandum, TM-FBR-77-43.